2010

Maximizing the Life of a Lithium-Ion Cell by Optimization of Charging Rates

Saeed Khaleghi Rahimian
University of South Carolina, khaleghi@email.sc.edu

Sean Rayman
University of South Carolina - Columbia, rayman@cec.sc.edu

Ralph E. White
University of South Carolina - Columbia, white@cec.sc.edu

Publication Info

Published in *Journal of the Electrochemical Society*, Volume 157, Issue 12, 2010, pages A1302-A1308.

Journal of The Electrochemical Society, **157** (12) A1302-A1308 (2010)
0013-4651/2010/157(12)/A1302/7/$28.00 © The Electrochemical Society

Maximizing the Life of a Lithium-Ion Cell by Optimization of Charging Rates

Saeed Khaleghi Rahimian,* Sean C. Rayman,* and Ralph E. White,z**

Department of Chemical Engineering, University of South Carolina, Columbia, South Carolina 29208, USA

Using a dynamic optimization method, the optimum charge currents as a function of cycle number during cycling for the lithium-ion cell are obtained. A single particle physics-based model, which includes capacity fade, was applied to simulate the cell performance under low earth-orbit (LEO) cycling conditions. Useful cell life is defined as the number of cycles before the end of discharge voltage drops below 3.0 V or the cell discharge capacity becomes less than 20% of the original discharge capacity. The simulated useful cell life can be increased by ~29.28% by varying the charge current.
 [DOI: 10.1149/1.3491367]

Manuscript submitted June 21, 2010; revised manuscript received August 30, 2010. Published October 6, 2010.

The useful life of lithium-ion cells is of interest for many applications. A substantial amount of work has been done to understand the capacity fade phenomena and predict the battery life.[1-22] However, only a few tried to determine the effect of cycling conditions on capacity fade and cell life.[18-22] For example Ramadass et al. studied the influence of the end of charge voltage (EOCV) and depth of discharge (DOD) on capacity loss.[18] They observed that reducing the EOCV and the DOD for possible application can result in smaller capacity fade and increased cycle life. A new varying current decay (VCD) protocol with faster charge rate was developed by Sikha et al. to compare the capacity fade of a lithium-ion cell with conventional constant current–constant voltage (CC-CV) and CV protocols.[19] Because of the small increase in the potential above the cutoff value, higher impedance for the cells cycled using the VCD protocol was observed compared to the CC-CV protocol. Lee et al. showed the effect of the different EOCV, DOD, and charging rates on a cell life under low earth-orbit (LEO) cycling conditions.[20] They obtained similar results as Ramadass et al.;[18] the useful life of the cell can be extended by reducing EOCV and DOD, which reduces the rate of the side reaction. None of the above works optimize the cell life by applying an optimization routine. Recently, Methekar et al.[21] used the dynamic optimization method to find the best charging profile for lithium-ion batteries to maximize the energy storage. However, Methekar et al. did not deal with the useful cell life. Similar work has been done by Wang to maximize the efficiency of the battery charging process, which is defined as the ratio of the energy accumulated in the battery over the actual energy supplied to it.[22] The optimal current profile during charging was obtained by using optimal control theory techniques and the energy loss compared with the conventional CC-CV protocol.

In this paper, lithium-ion cell life is maximized for LEO cycling by optimizing the charging current using dynamic optimization.

Model

The single particle (SP) model was used because it is less computationally intensive than the pseudo-two-dimensional (P2D) model.[23] The SP model, which includes capacity fade, was applied to predict the cell life for low discharge rates (one C rate or less).[23] The assumptions associated with the SP model are as follows:

1. The concentration of the electrolyte is constant and uniform for all time across the cell sandwich (cathode, separator, and anode).
2. The potential in the solution phase is constant and uniform for all time across the cell.
3. Positive and negative electrode potentials depend on time only.
4. The side reaction is the reduction of ethylene carbonate (EtCO) expressed as[24]

$$S + 2Li^+ + 2e^- \rightarrow P$$

where S and P are the solvent and the product, respectively.

5. The side reaction does not occur during the discharge.
6. The lithium deposition side reaction is not considered.

The mathematical formulation of the SP model is presented in Appendix A. The capacity fade parameters (e.g., i_{0f}) are set to exaggerate the rate of reduction of EtCO, thus decreasing the cell life and computation time by reducing the number of cycles that must be simulated to achieve end of life. The parameters used in this model are given in Table I.

LEO cycling, which contains the following steps, was applied for the cell simulation after the cell is completely charged initially.

1. CC discharge [0.6857 C rate (40% DOD)] for 35 min discharge time. Unless the voltage drops below 3.0 V or the cell capacity reaches 20% of the total discharge capacity, go to step 2.
2. CC charging (up to 1 C rate) for 61 min charge time. If the voltage reaches the EOCV (4.05 V), go to step 2, if not, go to step 3.
3. CV (4.05 V) charging for the remaining charge time, go to step 1.

Dynamic Optimization

The dynamic optimization problem is simply defined as

$$\max_{u(t)} \; J = \phi[x(t_f)]$$

$$s \cdot t\frac{dx}{dt} = F(x,y,u,p), \quad x(0) = x_0$$

$$0 = G(x,y,u,p)$$

$$u_L \leq u(t) \leq u_U$$

where x is the differential state variable vectors with the initial condition of x_0, y is the vector of algebraic variables, u is the control variable vector (input), p is the vector of parameters, and J is the objective function value, which is evaluated at the final time (t_f). In the SP model, x is a vector containing $[x_{p,avg}, x_{n,avg}, \delta_{film}]$, y vector is $[x_{p,surf}, x_{n,surf}, \phi_p, \phi_n, V_{cell}]$, u is the charge current (I_{app}), p is a vector of constant parameters, and ϕ function is defined as follows

$$\phi[x(t_f), y(t_f), u, p] = N_{cycle} + \alpha_{cycle}$$

where N_{cycle} is the total number of cycles at which the end of discharge voltage (EODV) remains above 3.0 V and the cell capacity is at least 20% of the total capacity of the cell. α_{cycle} is defined in the next section.

In this work, the sequential approach (partial discretization),[25] which converts the dynamic optimization problem to a nonlinear programming (NLP), is applied in the following manner: To use the

* Electrochemical Society Student Member.
** Electrochemical Society Fellow.
z E-mail: white@cec.sc.edu

Table I. Model parameters.

Parameter	Value	Unit
Exchange current density for the film formation reaction (i_{0f})	1×10^{-10}	A/cm^2
Molecular weight of film (M_f)	74	g/mol
Film specific conductivity (k_f)	5×10^{-8}	S/cm
OCP for film formation reaction ($U_{ref,f}$)	0.4	V
Film density (ρ_f)	2.1	g/cm^3
Anode rate constant (k_n)	0.4854	A cm$^{2.5}$/mol$^{1.5}$
Cathode rate constant (k_p)	0.2252	A cm$^{2.5}$/mol$^{1.5}$
Electrolyte concentration (c_e)	1×10^{-3}	mol/cm^3
Anode maximum solid phase ($c_{n,max}$)	0.030555	mol/cm^3
Cathode maximum solid phase ($c_{p,max}$)	0.051555	mol/cm^3
Anode radius particle (R_n)	2×10^{-4}	cm
Cathode radius particle (R_p)	2×10^{-4}	cm
Anode solid phase diffusion coefficient of Li$^+$ ($D_{s,n}$)	1×10^{-10}	cm^2/s
Cathode solid phase diffusion coefficient of Li$^+$ ($D_{s,p}$)	3.9×10^{-10}	cm^2/s
Resistance of the SEI layer (R_{SEI})	1×10^{-6}	Ω cm^2
Cell resistance (R_{cell})	0.02	Ω
Initial cell capacity (Q_0)	1.3387	Ah
Anode electroactive surface area (S_n)	4×10^4	cm^2
Cathode electroactive surface area (S_p)	4×10^4	cm^2
Anode initial state of charge (θ_0^n)	0.03	—
Cathode initial state of charge (θ_0^p)	0.95	—
Cathodic transfer coefficient for the film formation reaction ($\alpha_{c,f}$)	0.5	—
Cathodic transfer coefficient ($\alpha_{a,i}$)	0.5	—
Anodic transfer coefficient ($\alpha_{c,i}$)	0.5	—
Temperature (T)	298.15	K
Gas constant (R)	8.3143	J/mol/K
Faraday's constant (Far)	96,487	C/mol

different charge currents during cycling, the total number of cycles must be known. However, the total number of cycles is not known a priori. Therefore, the total number of cycles obtained for one optimal charge rate is rounded up to 320, the nearest product of 5 and the set 2^k, the number of decision variables where k is up to 6. The procedure starts with dividing the assumed total number of cycles (320) by N, which are equally spaced cycle number subdomains and then using a constant charge rate for each subdomain. Thus, instead of applying a constant charge current during the entire cell life, different charge rates were used for cycling.

To solve the NLP resulting from the sequential dynamic optimization method, MATLAB Genetic Algorithm and Direct Search Toolbox[26] was used. To make the optimization algorithm more efficient, both the direct search method and the genetic algorithm were used in this work as follows: To increase the objective function rapidly, first, the direct search approach was applied. Then, the resulting point was considered as one of the children for the initial population in the genetic algorithm. If the objective function was improved by the genetic algorithm, the procedure is repeated; otherwise, the optimization algorithm stops. The optimization flowchart is shown in Fig. 1. To validate the efficiency of the optimization routine, some typical optimization problems containing local optimum points were solved and the results are shown in Appendix B.

Results and Discussion

The objective function, the number of cycles, has discrete values. Therefore, a continuous term called the cycle fraction was added to make the objective function a continuous function. A continuous objective function improves the efficiency of the optimization algorithm, especially for the direct search method. The cycle fraction is defined as

$$\alpha_{cycle} = \frac{\text{cell capacity remaining after last full cycle}}{\text{minimum cell capacity allowed}}$$

The minimum cell capacity allowed is one of the constraints for stopping the cell cycling. In this work, the minimum EODV constraint always determines the useful cell life, and the minimum cell capacity is always greater than 20% of the original discharge capacity at the last cycle. So the value of α_{cycle} is always greater than 1.

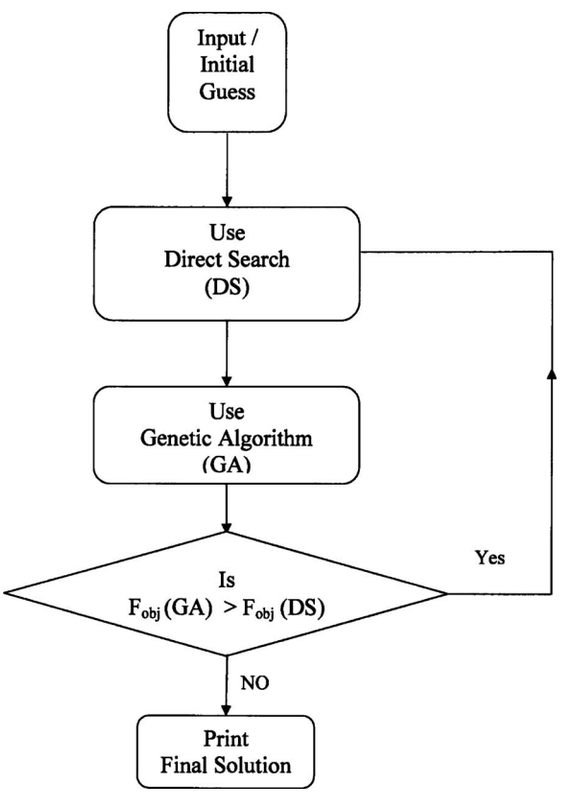

Figure 1. Optimization algorithm.

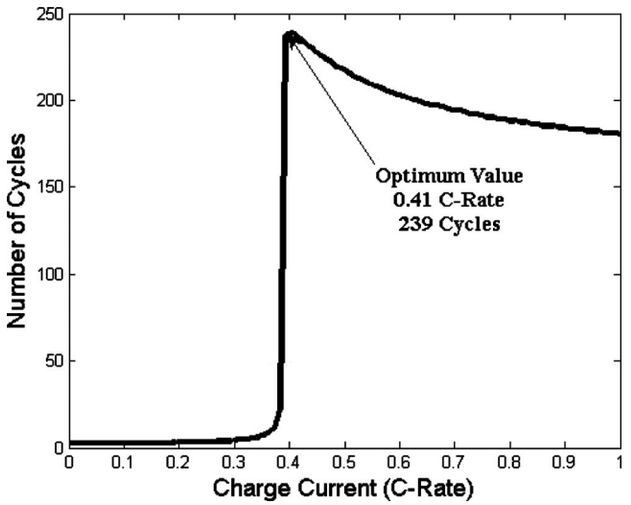

Figure 2. Number of cycles vs charge current for single charge current.

The first cycle is used to calculate the initial cell capacity. The cell is first charged with CC until the cell voltage reaches the EOCV and then CV charging (4.05 V) is applied until the current drops below 0.001C rate. The first cycle remains the same in the optimization process and the variable charging rates are applied for cycles greater than 1.

To show how the number of cycles changes with a single charge current, Fig. 2 is provided. The number of cycles increases rapidly with the charge current before the maximum and then decreases smoothly. Using low charge current makes the cell capacity and the EODV decrease rapidly with the number of cycles. A higher charge current enhances the side reaction rate and, as a result, we would have less useful life. Therefore, the demand for an optimization problem arises to seek the best charge current to maximize the cell life.

At first, only a single charge current for dynamic optimization is used, so in this case, the control vector contains only one variable. The maximum value for the objective function obtained was 239 and the optimum current is 0.4055C rate. Figures 3-5 show the cell capacity, the EODV, and the EOCV vs the cycle number, respectively. The data in Fig. 4 indicate that the EODV constraint determined the cell life. Using two charge currents, the first one is applied for the cycles below 160 (the total number of cycle is assumed to be 320 cycles, as mentioned above) and the second current is used

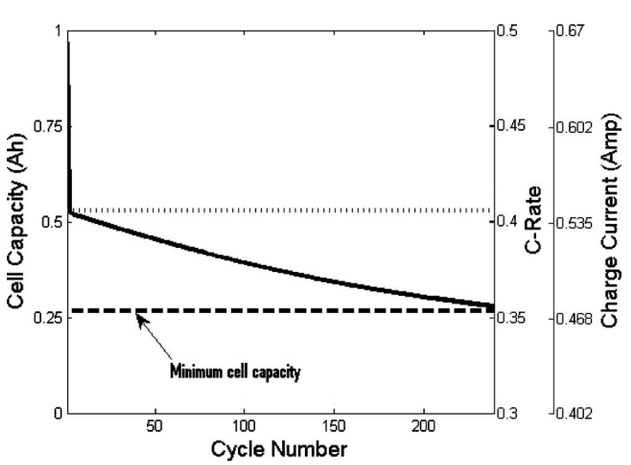

Figure 3. Cell capacity vs cycle number for single charge current.

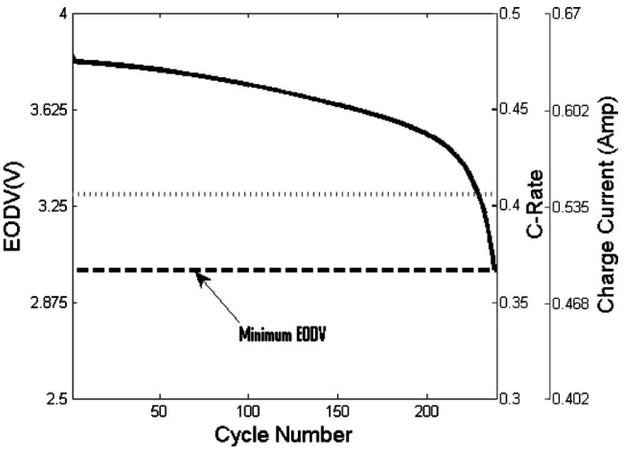

Figure 4. EODV vs cycle number for single charge current.

for the remaining cycles. The optimum values obtained for the charge rates are 0.3924 and 0.4152 C rate, respectively; the objective function increases to 255. The cell capacity, the EODV, and the EOCV vs the cycle number are shown in Fig. 6-8, respectively. Because there is no constraint to keep the EOCV for all the cycles at 4.05, in some cycles, the EOCV value is less than 4.05 V.

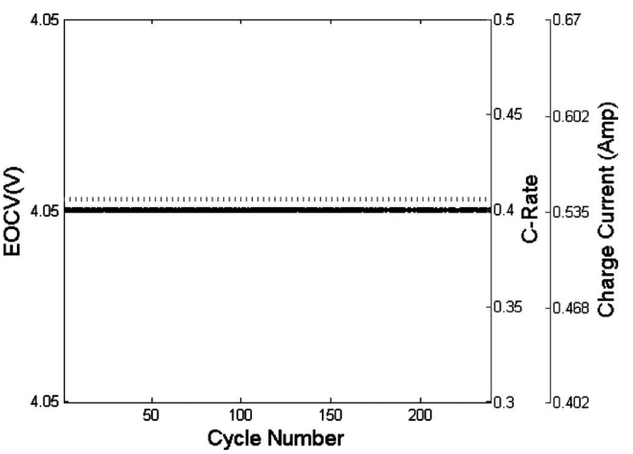

Figure 5. EOCV vs cycle number for single charge current.

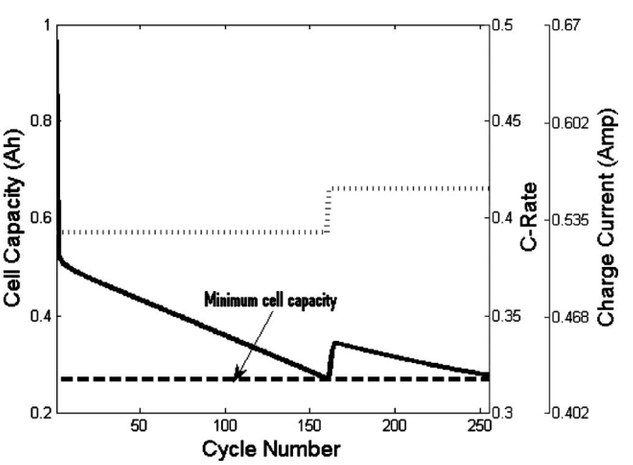

Figure 6. Cell capacity vs cycle number for two charge currents.

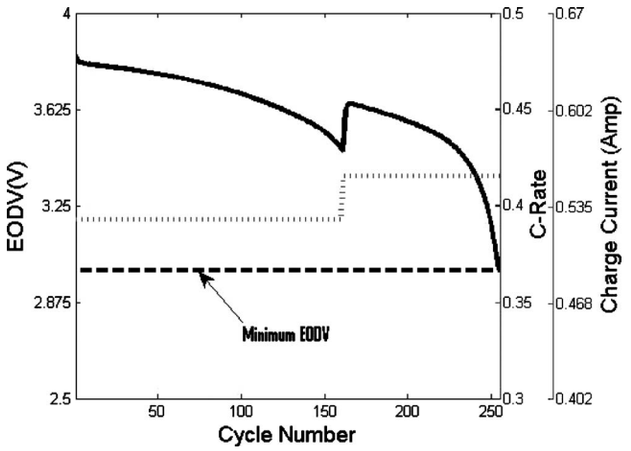

Figure 7. EODV vs cycle number for two charge currents.

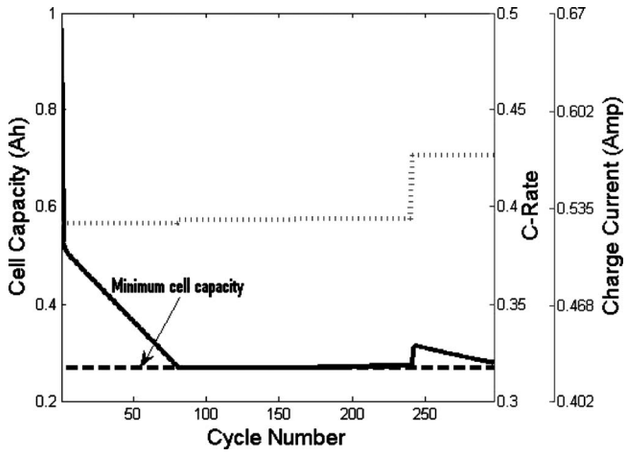

Figure 9. Cell capacity vs cycle number for four charge currents.

Choosing four different charge currents increases the cell life by ~24.26% with respect to the case when single optimum charge current is used. The objective function value for the four optimum currents is 297, and the results for the cell capacity, the EODV, and the EOCV are shown in Fig. 9-11, respectively. The important observation is that the last current $[I_{app}(4)]$, which is applied in cycles greater than 240, is much higher than the previous current $[I_{app}(3)]$. This event is because the EOCV reaches 4.05 V during these cycles and, consequently, the EODV begins to drop below 3.0 after cycle 287 if the current remains constant $[I_{app}(3) = I_{app}(4)]$, as shown in Fig. 12. Therefore, to avoid this situation, the charge current must increase. However, any value more than the obtained value causes the capacity to drop more rapidly and, as a result, the cell life decreases. The optimization results for different numbers of charge currents are summarized in Table II. Improvement of the objective function is not a monotonic function of the number of charge currents. This would occur if we kept dividing the number of cycles from the same initial number. (e.g., 2, 4, 8, … or 5, 10, 20, …).

The last plots are for the maximum number of charge currents we applied. The number of cycles increases to ~29.28% with respect to one optimum current by choosing 20 decision variables and the objective function value at the optimum point is 309. Figures 13-15 show the capacity cell, the EODV, and the EOCV, respectively, at the optimum charge rates. Because using 20 decision variables does not enhance the objective function with respect to the case with 10 decision variables, we decided to stop the optimization at this number of variables.

To make sure that the cell capacity balancing constraint is satisfied during the cycling, the cell capacity balance for every 15 cycles (daily basis) is shown in Fig. 16. Because 40% of DOD is kept constant during the cycling, the total discharge capacity through 15

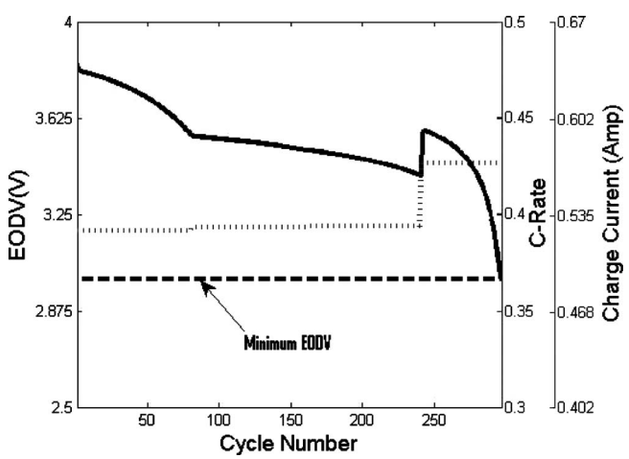

Figure 10. EODV vs cycle number for four charge currents.

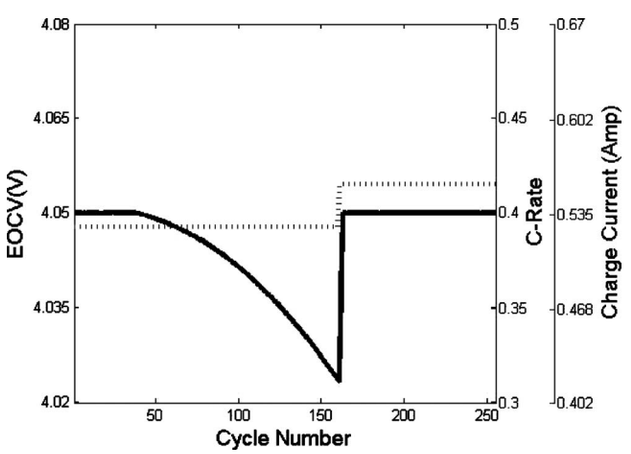

Figure 8. EOCV vs cycle number for two charge currents.

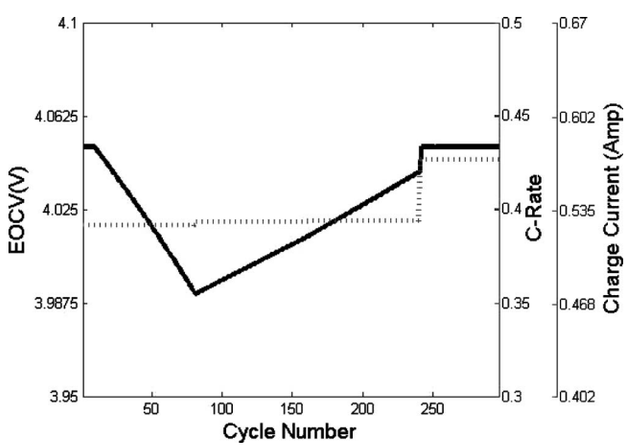

Figure 11. EOCV vs cycle number for four charge currents.

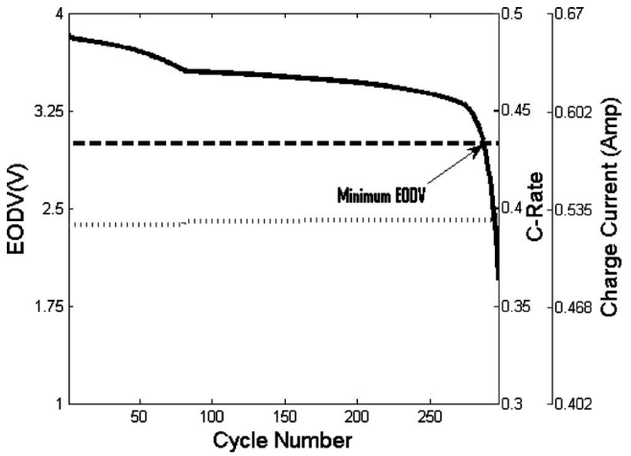

Figure 12. EODV vs cycle number for four charge currents [$I_{app}(4) = I_{app}(3)$].

Table II. Dynamic optimization results.

Number of charge currents	Objective function value	Percent increase with respect to the case with one charge current	Number of objective function evaluations
1	239.043741	0	957
2	255.036768	6.6904	4354
4	297.045917	24.2643	11,274
5	305.043895	27.6101	11,522
8	306.038250	28.0260	42,883
10	309.038612	29.2812	20,641
16	306.038768	28.0263	45,441
20	309.038792	29.2813	80,801

cycles remains at the value of 8.0322 Ah ($15 \times 0.4 \times Q_0$). In the figure, the total charge capacity is in the range of $(-0.83 + 3.21)\%$ of the total discharge capacity.

Conclusion

The life of the lithium-ion cell can be maximized by applying different charge rates during cycling. To avoid a decrease in the cell capacity, the charge currents needs to be kept at higher values. However, increasing the charge rates causes more capacity fade and shorter cell life. Therefore, there is an optimum charge current profile that was obtained in this work by using the dynamic optimization framework, which results in an estimate increase in useful cell life of ~30%.

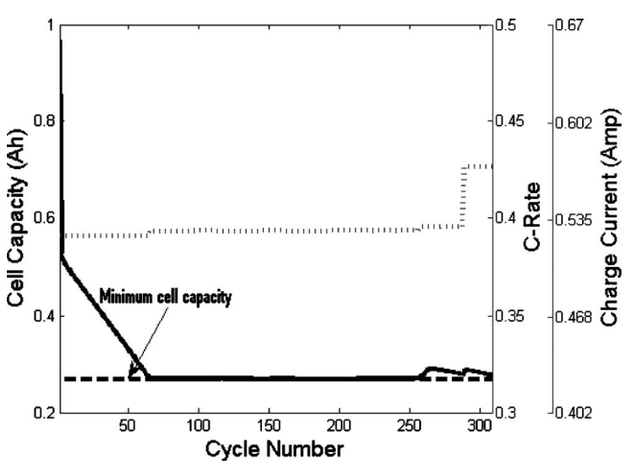

Figure 13. Cell capacity vs cycle number for 20 charge currents.

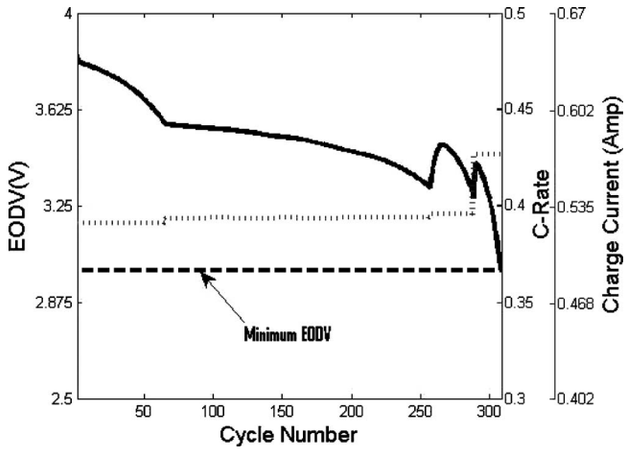

Figure 14. EODV vs cycle number for 20 charge currents.

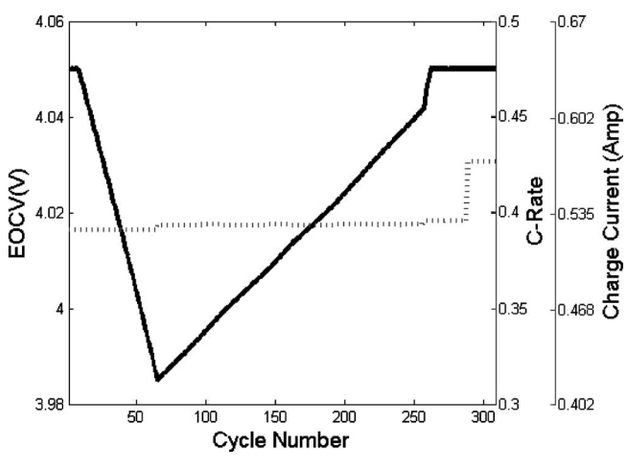

Figure 15. EOCV vs cycle number for 20 charge currents.

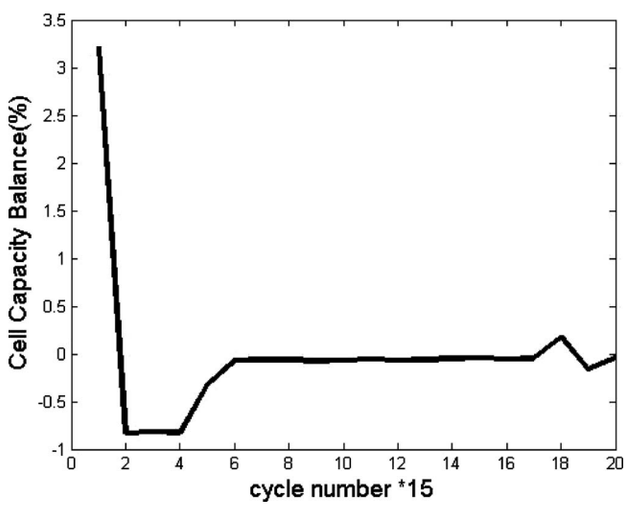

Figure 16. Cell capacity balance (daily basis) for 20 charge currents.

University of South Carolina assisted in meeting the publication costs of this article.

Appendix A

Fick's second law (partial differential equation), by applying a volume average technique, is simplified to predict the diffusion of the lithium ions in a spherical particle. This form contains ordinary differential equation and algebraic constraint equation with the variables $x_{i,avg}$ and $x_{i,surf}$ (i = p,n) for each of the electrodes together with their initial conditions. For the cathode, we have

$$\frac{dx_{p,avg}}{dt} = \frac{-3J_p}{\mathrm{Far}R_p c_{p,max}}$$

$$x_{p,surf} - x_{p,avg} = \frac{-J_p R_p}{5\mathrm{Far}D_{s,p}c_{p,max}}$$

$$J_p = \frac{I_{app}}{S_p}$$

The above equations for the anode are the same as those for the cathode but include the side reaction (only during charge) as below

$$\frac{dx_{n,avg}}{dt} = \frac{-3J_n}{\mathrm{Far}R_n c_{n,max}}$$

$$x_{n,surf} - x_{n,avg} = \frac{-J_n R_n}{5\mathrm{Far}D_{s,n}c_{n,max}}$$

$$J_n = \frac{-I_{app}}{S_n} - J_s$$

where $x_{i,avg}$ is the ratio of the solid average concentration to the maximum solid concentration for each electrode ($c_{i,max}$), $x_{i,surf}$ is the ratio of the solid surface concentration to the maximum solid concentration, which is equal to the state of charge (SOC) for each electrode.

J_s, the side reaction rate expression, is calculated by using cathodic Tafel kinetics by assuming that the irreversible reaction and the amount of lithium deposited is very small and reacts quickly with the solvent[2]

$$J_s = -i_{0f}\ \exp\left(\frac{-\alpha_{c,f}\mathrm{Far}}{RT}\eta_s\right)$$

where η_s, the side reaction overpotential, is expressed as

$$\eta_s = \phi_n - U_{ref,f} - \frac{I_{app}}{S_n}R_{film}$$

R_{film} is defined as

$$R_{film} = R_{SEI} + \frac{\delta_{film}}{k_f}$$

where SEI is solid electrolyte interphase and the rate at which the film thickness increases is calculated by[18]

$$\frac{d\delta_{film}}{dt} = \frac{-J_s M_f}{\rho_f Far}$$

The Butler–Volmer kinetic expression is used to predict the rates of lithium-ion deintercalation and intercalation reactions for each electrode as

$$J_i = k_i(c_{i,max} - x_{i,surf}c_{i,max})^{0.5}(x_{i,surf}c_{i,max})^{0.5}c_e^{0.5}\left[\exp\left(\frac{\alpha_{a,i}\mathrm{Far}}{RT}\eta_i\right) - \exp\left(\frac{-\alpha_{c,i}\mathrm{Far}}{RT}\eta_i\right)\right]$$

The overpotentials for the lithium-ion intercalation reaction for the anode and the cathode are given as

$$\eta_p = \phi_p - U_p^{\theta}$$

$$\eta_n = \phi_n - U_n^{\theta} \mp \frac{I_{app}}{S_n}R_{film}\left(\begin{Bmatrix} -\text{ charge} \\ +\text{ discharge}\end{Bmatrix}\right)$$

The open-circuit potentials (OCP) as functions of the SOC for the carbon anode and the cathode ($LiCoO_2$ with no Ni) are expressed as

$$U_n(\theta_n) = 0.7222 + 0.1387\theta_n + 0.029\theta_n^{1/2} - \frac{0.0172}{\theta_n} + \frac{0.0019}{\theta_n^{1.5}} + 0.2808 \times 10^{(0.9-15\theta_n)} - 0.7984 \times 10^{(0.4465\theta_n - 0.4108)}$$

$$U_p(\theta_p) = \frac{-4.656 + 88.669\theta_p^2 - 401.119\theta_p^4 + 342.909\theta_p^6 - 462.471\theta_p^8 + 433.434\theta_p^{10}}{-1 + 18.933\theta_p^2 - 79.532\theta_p^4 + 37.311\theta_p^6 - 73.083\theta_p^8 + 95.96\theta_p^{10}}$$

The cell voltage is obtained by the equation

$$V_{cell} = \phi_p - \phi_n + I_{app}R_{cell}$$

The model considers capacity fade by incorporating the side reaction rate (J_s) and the film resistance (R_{film}) into the equations. Moreover, the SOC of the positive electrode updated at the end of each charging process is as follows[18]

$$\theta_{p,N} = \theta_{p,N-1} - \theta_{1,N-1}$$

where θ_1 is the loss of SOC obtained by dividing the capacity loss to the maximum capacity of the cell

$$\theta_1 = \frac{Q_S}{Q_{max}}$$

$$Q_s = -\int_0^{t=t_{CC+CV}} (J_s S_n)dt$$

$$Q_{max} = \int_0^{t=t_{CC+CV}} I_{app}dt \quad (N = 1)$$

The charge capacity is calculated for each cycle as

$$Q_p = \int_0^{t=t_{CC+CV}} I_{app}dt$$

The cell capacity at each cycle is obtained by the following formula

$$Q_N = Q_0 + \sum_{i=2}^{N_{cycle}} [Q_p(i) - Q_{dis}(i)]$$

Q_0, the initial cell capacity, is calculated by initially charging the cell at CC until the cell voltage reaches 4.05 V, held potentiostatic until the current drops below 0.001 C rate, and discharged at the same constant charge rate. Because the discharge rate and time are constant during cycling, Q_{dis} does not change during simulation.

Appendix B

The first example is to find the global minimum of the Colville function as follows[27]

$$f(x) = 100(x_1^2 - x_2)^2 + (x_1 - 1)^2 + (x_3 - 1)^2 + 90(x_3^2 - x_4)^2 + 10.1[(x_2 - 1)^2 + (x_4 - 1)^2] + 19.8(x_2 - 1)(x_4 - 1) - 10 \le x_i \le 10, \quad i = 1, \cdots, 4$$

The global minimum is $x^* = (1.0,1.0,1.0,1.0)$, $f(x^*) = 0.0$. The results for using the direct search method, genetic algorithm, and our approach, which is the combination of both methods, are given in Table B-I. The initial point is chosen as $x^0 = (5.0,5.0,5.0,5.0)$ for the direct search method and one of the children in the initial population of the genetic algorithm.

The maximum generation for the genetic algorithm was considered unlimited, but in our approach, this value is set to $100 \times N$, where N is the number of decision variables. So for this problem, the maximum number of generations is 400. Other parameters in the direct search and genetic methods are the same as our approach.

The second example was chosen as the constrained optimization with the following equations[27]

$$\max f(x) = \frac{\sin^3(2\pi x_1)\sin(2\pi x_2)}{x_1^3(x_1 + x_2)}$$

$$s \cdot tg_1(x) = x_1^2 - x_2 + 1 \le 0$$

$$g_2(x) = 1 - x_1 + (x_2 - 4)^2 \le 0$$

$$0 \le x_i \le 10, \quad i = 1,2$$

$x^* = (1.22979713,4.2453733)$, $f(x^*) = 0.095825$, is the global maximum, and the optimization results for the three different methods are presented in Table B-II. $x^0 = (5.0,5.0)$ was selected as the initial point.

Table B-I. Optimization results for the Colville function.

Algorithm	Number of function evaluations	Algorithm output
Direct search	3160	5.61315
Genetic	198,540	0.0002465
Our approach	65,738	1.563×10^{-5}

Table B-II. Optimization results for the constrained optimization.

Algorithm	Number of function evaluations	Algorithm output
Direct search	70	1.07138×10^{-17}
Genetic	40,244	0.0291438
Our approach	38,296	0.095825

List of Symbols

c_e electrolyte concentration, mol/cm^3
$c_{i,max}$ maximum solid phase for each electrode (i = p,n), mol/cm^3
$D_{s,i}$ solid phase diffusion coefficient of Li^+ or each electrode (i = p,n), cm^2/s
F system of differential equations
Far Faraday's constant, C/mol
G system of algebraic equations
i_{0f} exchange current density for the film formation reaction, A/cm^2
I_{app} applied current, C/s
J objective function value
J_s side reaction rate expression, C/s
k number of decision variables
k_f film specific conductivity, S/cm
k_i rate constant for each electrode (i = p,n), A cm$^{2.5}$/mol$^{1.5}$
M_f molecular weight of film, g/mol
N_{cycle} total number of cycles
p parameter vector
Q_0 initial cell capacity, Ah
Q_{dis} discharge capacity, Ah
Q_{max} maximum capacity of the cell, Ah
Q_N cell capacity at each cycle, Ah
Q_p charge capacity, Ah
Q_S capacity loss, Ah
R gas constant, J/mol/K
R_{cell} cell resistance, Ω
R_{film} film resistance, Ω cm^2
R_i radius particle for each electrode (i = p,n), cm
R_{SEI} resistance of the SEI layer, Ω cm^2
S_i electroactive surface area for each electrode (i = p,n), cm^2
t_f final time, s
T temperature, K
u control variable vector
U_i^θ OCP for each electrode (i = p,n), V
$U_{ref,f}$ OCP for film formation reaction, V
V_{cell} cell voltage, V
x differential state variable vectors
x_0 initial condition of the state variable vectors
$x_{i,avg}$ ratio of the solid average concentration to the maximum solid concentration for each electrode (i = p,n)
$x_{i,surf}$ ratio of the solid surface concentration to the maximum solid concentration for each electrode (i = p,n)
y algebraic variable vector

Greek

$\alpha_{a,i}$ cathodic transfer coefficient
$\alpha_{c,i}$ anodic transfer coefficient
$\alpha_{c,f}$ cathodic transfer coefficient for the film formation reaction
α_{cycle} cycle fraction
δ_{film} film thickness, cm
η_i overpotentials for the lithium-ion intercalation reaction for each electrode (i = p,n), V
η_s side reaction overpotential, V
θ_0^i initial SOC for each electrode (i = p,n)
θ_1 loss of SOC
ρ_f film density, g/cm^3
ϕ objective function
ϕ_i potential reaction for each electrode (i = p,n), V

References

1. R. Darling and J. Newman, *J. Electrochem. Soc.*, **145**, 990 (1998).
2. P. Arora, R. E. White, and M. Doyle, *J. Electrochem. Soc.*, **146**, 3543 (1999).
3. H. Cao, J. Yu, L. Kang, H. Yang, and X. Ai, *Comput. Chem. (Oxford)*, **25**, 251 (2001).
4. A. Urbina, T. L. Paez, R. G. Jungst, and B. Y. Liaw, *J. Power Sources*, **110**, 430 (2002).
5. R. B. Wright, C. G. Motloch, J. R. Belt, J. P. Christophersen, C. D. Ho, R. A. Richardson, I. Bloom, S. A. Jones, V. S. Battaglia, G. L. Henriksen, et al., *J. Power Sources*, **110**, 445 (2002).
6. R. Spotnitz, *J. Power Sources*, **113**, 72 (2003).
7. J. Christensen and J. Newman, *J. Electrochem. Soc.*, **150**, A1416 (2003).
8. R. G. Jungst, G. Nagasubramanian, H. L. Case, B. Y. Liaw, A. Urbina, T. L. Paez, and D. H. Doughty, *J. Power Sources*, **119–121**, 870 (2003).
9. I. Bloom, S. A. Jones, V. S. Battaglia, G. L. Henriksen, J. P. Christophersen, R. B. Wright, C. D. Ho, J. R. Belt, and C. G. Motloch, *J. Power Sources*, **124**, 538 (2003).
10. B. Yann Liaw, G. Nagasubramanian, R. G. Jungst, and D. H. Doughty, *Solid State Ionics*, **175**, 835 (2004).
11. K. T. Chau, K. C. Wu, and C. C. Chan, *Energy Convers. Manage.*, **45**, 1681 (2004).
12. B. Y. Liaw, R. G. Jungst, G. Nagasubramanian, H. L. Case, and D. H. Doughty, *J. Power Sources*, **140**, 157 (2005).
13. A. T. Stamps, C. E. Holland, R. E. White, and E. P. Gatzke, *J. Power Sources*, **150**, 229 (2005).
14. M. Dubarry and B. Y. Liaw, *J. Power Sources*, **174**, 856 (2007).
15. E. V. Thomas, I. Bloom, J. P. Christophersen, and V. S. Battaglia, *J. Power Sources*, **184**, 312 (2008).
16. M. Safari, M. Morcrette, A. Teyssot, and C. Delacourta, *J. Electrochem. Soc.*, **156**, A145 (2009).
17. M. Zackrisson, L. Avellán, and J. Orlenius, *J. Cleaner Prod.*, **18**, 1519 (2010).
18. P. Ramadass, B. Haran, P. M. Gomadam, R. E. White, and B. N. Popov, *J. Electrochem. Soc.*, **151**, A196 (2004).
19. G. Sikha, P. Ramadass, B. Haran, R. E. White, and B. N. Popov, *J. Power Sources*, **122**, 67 (2003).
20. J. Lee, Y. K. Anguchamy, and B. N. Popov, *J. Power Sources*, **162**, 1395 (2006).
21. R. N. Methekar, V. Ramadesigan, R. D. Braatzb, and V. R. Subramanian, in *AIChE Annual Meeting* (2009).
22. J. Wang, in *SAE International*, Technical Paper 2010-01-1238 (2010).
23. C. R. Yang, Y. Y. Wang, and C. C. Wan, *J. Power Sources*, **72**, 66 (1998).
24. S. Santhanagopalan, Q. Guo, P. Ramadass, and R. E. White, *J. Power Sources*, **156**, 620 (2006).
25. V. S. Vassiliadis, Ph.D. Thesis, University of London, London, United Kingdom (1993).
26. http://www.mathworks.com/, last accessed October 5, 2010.
27. http://www-optima.amp.i.kyoto-u.ac.jp/member/student/hedar/Hedar_files/go.htm, last accessed October 5, 2010.